Journal of Solar Energy Research (JSER)

Journal homepage: www.jser.ut.ac.ir

Water Desalination and Power Generation Using a New and Innovative Single-slope Double-basin System

Mohammed Ajmi Abed[a,*], Naziha N. Aneizan[b], Falah Mohammed Abed[c]

[a]*College of Health and Medical Techniques Al-Dour, Northern Technical University, Iraq*
[b]*General Directorate of Education Salahaddin, Salahaddin, Iraq*
[b]*Al-Dour Technical Institute, Northern Technical University, Iraq*

ARTICLE INFO

Article Type:

Research Article

Received:2025.11.22
Accepted in revised form:2025.12.21

Keywords:
Solar still;
New desalination system;
Thermoelectric;
Voltage generation;
Productivity

A B S T R A C T

While solar stills represent a sustainable solution for water desalination, their practical application is often hindered by modest productivity rates. This study presents a novel design aimed to enhance daily productivity through a double-basin configuration with a single condensation surface that separates the two. Peltier units enhance the condensation process by transferring heat between the two basins while simultaneously generating power. The redesigned setup, utilizing the upper basin as a water source, enhanced water extraction by increasing the condensation rate on the glass surface, as determined by productivity, absorption temperature, and generated voltage. The maximum water yield was recorded between 12:00 PM and 1:00 PM, reaching approximately 0.479 L/hour, corresponding to a thermal gradient of about 17˚C. The daily yield was recorded at 0.8 L/day, 1.328 L/day, and 1.770 L/day for the system without the upper basin, with the Peltier unit basin, and with the Peltier unit basin coupled with a distillation basin, respectively. These results represent productivity enhancements of approximately 66% and 121%, respectively, indicating that the final modification significantly outperformed the conventional solar still by 221% in terms of overall daily output.

1. Introduction

Given the depletion of freshwater resources, the continuing global demand for it, and the accompanying climate change, especially in regions with persistent aridity, water and energy are the primary resources for sustaining life on this planet [1, 2]. Many water desalination devices have been developed and manufactured, but most of these devices and systems require energy to operate.

*Corresponding Author Email: mohammed.aj@ntu.edu.iq

Cite this article: Abed, M. Ajmi , Aneizan, N. N and Abed, F. Mohammed (2025). Water Desalination and Power Generation Using a New and Innovative Single-slope Double-basin System. Journal of Solar Energy Research, 10(4), 2616-2632. doi: 10.22059/jser.2025.406743.1670

DOI: 10.22059/jser.2025.406743.1670

Energy is mostly obtained from fossil fuels or nuclear energy, which contribute to environmental and health problems over time. The remaining energy comes from renewable energy sources such as solar, wind, wave, and tidal energy[3,4]. The percentage of water on Earth is approximately 71%, but 97% of that is saltwater, which is unsuitable for drinking or irrigation. The remaining 0.3% represents fresh water on our planet, including polar ice [5,6].The sun is the most abundant energy source. It can be harnessed for desalination purposes through the use of various solar thermal collectors.

Solar radiation is absorbed and converted into usable thermal energy. Desalination is a practical and revolutionary method for obtaining potable water in most regions of the world. There are two methods for achieving this: direct and indirect. The simplicity of this approach offers several advantages, including ease of manufacture, low maintenance costs, non-polluting, and environmental friendliness [7, 8].

Solar desalination is a method of extracting salt and dissolved solids from seawater or saline water using solar radiation to make the water suitable for drinking. The two ways (Evaporation and condensation) are considered basic principles of solar desalination methods. Solar radiation incident on the surface of the solar still is transmitted to the basin where sea water is stored.

In most cases, the basin is made with a black sheet to increase the absorptivity and reflect only a minor amount of radiation to the environment. Then, the solar radiation raises the salt water temperature, thereby initiating the evaporation process. The evaporated water condenses on the glass top cover, and the condensed droplets of water are collected in an outer container as fresh water.
The classification of solar desalination systems is determined by the amount of freshwater produced, and can be either small-scale, medium-scale, or large-scale [٩,١٠]. Solar distillation devices are simple devices that require no manufacturing difficulties or constraints, despite their low production yield. Researchers have investigated new innovative methods and designs to enhance solar still productivity and thermal performance by increasing the evaporation surface area or heat transfer. Studies on desalination devices have explored various designs to achieve optimal distillation capabilities and high yields [11, 12]

Sasongko et al. [13] designed a desalination system that included four electric Peltier units. A small, cubic container filled with water was placed, and the hot side of the Peltier units was connected to it on all four sides. The cold side of the units faced the wall of the other container, inside which the entire assembly was placed as a cylindrical condensing surface with a conical lid. It was observed that an increase in power supplied to the units results in a bigger temperature differential across the Peltier, hence augmenting the desalination process. At 40.5 watts, the temperature difference between the two sides was 70°C for the hot side and 60°C for the cold side.

Ashour et al. [14] utilized humidification and dehumidification using an evaporative pad with Peltier units for condensation. A Cledek 5090 cellulose pad was used to increase the moisture content of the air pumped over the brine. The Peltier units then removed the heat from the air, allowing condensation to occur on the cold side. Results showed that the best performance was achieved at 9 volts and an air velocity between 0.5 and 1.0 m/s. The daily water productivity was 1400 mL/day when it was hot and dry, and 1800 mL/day when it was cooler with high humidity

Al-Madhhachi et al. [15] used a 300 mL tank of sample water with connected tubes for bidirectional circulation.A Peltier distillation system was designed to heat and evaporate water using the hot side and condense the cold side through an attached heat sink placed inside the container. Results show a distilled water rate of 28.5 ml/h, with an energy consumption of 0.00114 kWh/ml for an evaporation chamber filled with 10 × 10 × 30 mm3 of salt water. Al-Madhhachi et al. [16] designed a basin from an aluminum chamber mounted above a water bath. The cold side of the Peltier unit is positioned on the outer surface of the chamber as a tilted condenser, and the hot side is connected to a water-based heat exchanger to circulate the cold water through it to release the heat absorbed by the unit. To ensure stability, the water basin was operated at a constant voltage of 40 volts and a current of 0.25 amps to maintain the temperature of water at 50°C, while the thermoelectric unit was operated at a constant voltage of 10 volts and a current of 2 amps to maintain the cold side of the unit at 28°C. Water production increased and reached its maximum value when the temperature increased from 40°C to 70°C.

Hasanzadeh et al. [17] constructed a water desalination system integrated with Peltier units to enhance the condensation and heating process through a power supply. A desalination tank was used, and a heat radiator was installed inside the tank, along with six Peltier units. The thermoelectric units were installed and connected to a voltage

source to operate in two modes: the first used the hot side to increase evaporation, and the second used both the hot and cold sides to simultaneously increase evaporation and condensation. The results showed that using only the hot side of the solar thermal electric system increased freshwater production by 41.56%, while the simultaneous use of both sides improved production by 89.04% compared to the passive setup.

The performance of the solar stills suffers from low thermal efficiency and a gradual reduction of solar energy input over time due to dust accumulation. In addition, the elevated temperature on the condensing surface will reduce the condensation process. There is a lack of effective utilization of the temperature difference between the condensation surface and the temperature of the hot basin. Although many studies have attempted to improve solar stills through different modifications, there remains a lack of a comprehensive approach that integrates multiple enhancement techniques. The present study focuses on the development of a single-slope basin system as a new and innovative design to tackle several challenges, including the absence of direct solar radiation for heating, which has led to issues mentioned previously. The new design addresses the low condensing rate by reducing the temperature of the condensing surface and simultaneously capitalizing on the thermal gradient to generate electrical power.

2. Thermal Performance Indicators

Thermal concentration is very important because it's the base factor for absorbed and transmitted heat. Figure 1 represents a schematic of the parabolic concentrator. Some equations describe the energy balance and parametric equations for the thermal absorber. The greatest influence lies in the concentration ratio of the reflected radiation and the geometric shape of the receiver. The concentration ratio is defined as the amount of solar radiation accumulated by a given solar concentrator. There are two concentration ratios [18, 19].

2.1. Optical Solar Concentration Ratio

It is the ratio between the incoming energy on the reflective surface (Isur) and to radiant energy that reaches the absorber (Irec)given in equation (1) [19]:

$$CR-Opt = \frac{I_{sur}}{I_{rec}} \quad (1)$$

Geometric Concentration Ratio (CR): It is the ratio between the concentrator aperture area (Aa) to the receiver area (Arec). This relationship is expressed by equation (2) [37]:

$$C = \frac{A_a}{A_{rec}} \quad (2)$$

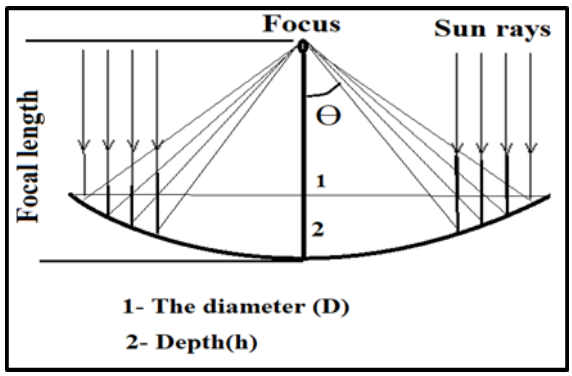

Figure 1. Schematic diagram of the geometrical parameters of the solar dish concentrator system

3. Peltier Device and Structure

A Peltier or thermoelectric power unit is a device designed to operate in reverse order, using cooling and heating. It can be used as an electrical power generator by the temperature difference of the two sides, or as a cooler for various applications by passing direct current through it. Each application differs in its implementation, requiring analysis based on data of thermal consumption, energy production, energy consumption, and economic costs [20,21].

A thermoelectric generator converts heat into electrical energy through the Seebeck effect. When two different conductors form a closed circuit through connections maintained at different temperatures, an electromotive force (EMF) is generated, resulting in an electric current.

This property can be employed for solar energy applications, heat from fuel cells, waste incineration, industrial dryers, and heat from automobile exhaust [22,23]. A Thermoelectric module is electrically arranged by two thermoelectric pairs (N–type and P-type semiconductor pellets) that are thermally equal. Ceramic plates are surrounded by semiconductor pairs. Thermoelectric semiconductor materials are alloys of Bismuth Telluride; most thermoelectric materials are accessible alloys for various applications, such as (PbTe, SiGe, and Bi-Sb) pairs [24,25]. The common semiconductor material with

dissimilar electron density is Bismuth Telluride (Bi_2Te_3). This module contains pellets of the Bi_2Te_3 semiconductor that are electrically coupled in a serial configuration consisting of both P-type and N-type elements semiconductors, but aligned in a parallel manner with respect to heat transfer [26]. The outer shell of the pelletizer is made of a ceramic material, most commonly aluminum oxide, which boasts excellent mechanical properties, as well as acting as an electrical insulator and having a good thermal conductivity [27].

4. Materials and Methods

4.1. Desalination System

The experimental investigation aims to examine the effect of incorporating an upper water basin for the lower basin, while cooling the condensation surface that separates the two basins, and simultaneously utilizing the temperature gradient to generate electricity. The experiment parts used in this study are displayed in Figure 2. The geometric dimensions of the basin, its size, and the slope of the collection surface affect the effectiveness of a single–basin solar still, as shown in earlier research [28, 29]. A larger basin enhances the volume of collected water per operational cycle, whereas a higher inclination angle of the condensing surface promotes a more efficient flow of the water into the collection basin. This configuration of solar stills offers several notable advantages, including low cost and ease of construction for domestic applications. In the present study, a parabolic dish concentrator was employed and fabricated from steel and covered with flexible glass mirrors possessing a reflectivity of 95%. These mirrors were precisely cut into appropriately sized pieces and attached to the concentrator surface using a high-adhesion glue. Table 1 represents the geometric dimensions of the parabolic concentrator.

Table1.Geometric information of the parabolic concentrator

Geometric Parameters	Value
Diameter of (PD) (d)	1.12m
Surface Collection of the parabola	$0.98m^2$
Focal distance (f)	71cm
Depth of parabola (h)	11cm
Rim angle	47
f/d	63.4cm

The receiver consists of a copper tube with an inner diameter of 1 cm, wrapped in rings with a diameter of 14 cm. It is extending for a distance of 50 cm before entering the heating basin. The system operates under a natural circulation, the receiver entering the heating basin for 15 cm in a U-shape configuration before exiting outward. Where the water passes through the pipe from the receiver into the basin and then exits from the other direction, and thus the process is repeated with an increase in the absorbed heat. The experiment is conducted at (8:00 AM to 3:30 PM) over three consecutive days (28-30 of August).

The heating element was placed inside a container filled with glass wool and covered with raw aluminum foil to prevent heat dissipation to the surroundings. The heating basin was constructed from galvanized iron with dimensions of (70 x 45 cm), a lower edge height of 15 cm, and an upper edge height of 50 cm. The same structure was applied to the upper basin, which was mounted on a glass base (condensing surface). The upper basin serves as a drainage unit, allowing water to flow downward to the lower basin as the water level drops. Figure 3 presents a simplified diagram of the solar still with its dimensions. To minimize heat losses from the hot basin to external ambient conditions, (5 cm) of insulation glass wool with a thermal conductivity of 0.045 W/m2 was positioned between the hot basin and the external insulating cover. Thermal silicone was used as a bonding material between the upper basin and the separator surface (condensing surface), as well as in the heating basin to prevent any possible leakage of liquids or vapor to the outside. Various instruments were employed to monitor the parameters affecting the solar still's performance. A temperature was measured with a laser thermometer with a scale between (-50 – 550 ˚C), as with a model of Benetech-Gm321, the temperature was measured at six points, and the temperature was compared with a calibrated thermocouple to determine the error rate, which did not exceed ±1°C. The temperature of the water in both the upper and lower basins is measured directly based on the temperature of the water surface, and the solar radiation device was (Sm 206-solar model with a specified error of ±10 W/m². As well as a wind speed measuring with an anemometer device (WT-816A). The generating voltage was measured with a multimeter device (DT-9205A model).

Figure 2. Experimental parts :(a) Upper basin (external water), (b) Hot basin, (C) Upper and hot basin, (d) concentrator, (e) Receiver, (f) Peltier units, (g) Experimental devices (laser thermometer for temperature data, Anemometer (air velocity), solar radiation device

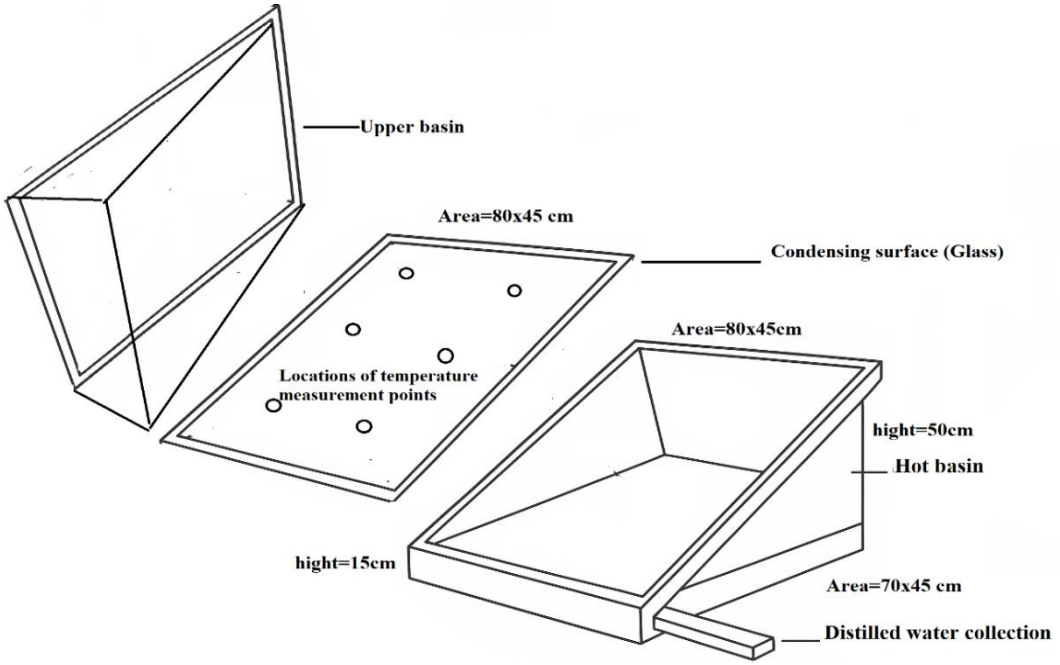

Figure 3. The double basin system of a solar still

4.2. Heat transfer analysis

Convection heat transfer can be divided into two principal types: steady transfer and transient transfer. Steady transfer refers to a condition in which the transfer rate remains unchanged with time, whereas transient transfer describes a state in which the transfer rate evolves and varies over time and is time-dependent. The steady-state heat transfer is not correlated with time derivatives, making it easier to handle. With certain assumptions, transfer can be reasonably treated as operating under steady state conditions. In a solar still, heat transfer can be categorized into two types: the internal processes and associated external interactions.

The internal heat transfer is the conversion of absorbed energy into increased temperature of the basin walls, brackish water, and phase change. The external transfer includes energy dissipation via the basin walls and the cooling effect on the outer surface of the basin's top cover. The thermal energy flux across a given surface by convection (q_{conv}) with respect to the data collected on the day, where (T_{Water}) denotes the temperature of water and (T_{Glass}) represents the temperature of glass, is calculated by equation (3) [30, 28]:

$$q_{conv} = hc\ A\left(T_{water} - T_{glass}\right) \quad (3)$$

The hourly exergy efficiency ($\eta_{exergy,\ hour}$) and the daily exergy efficiency ($\eta_{exergy,\ day}$) of the system are given by equations (4) and (5) [28]:

$$\eta_{exergy,hour} = Exergy_{out} / Exergy_{in} \quad (4)$$

$$\eta_{exergy,hour} = \Sigma Exergy_{out} / \Sigma Exergy_{in} \quad (5)$$

4.3. Heat transfer inside the solar still

a) The convective heat transfer: convection transfer between the water and the inner condensing surface /glass ($Q_{c,wg}$) caused by the temperature gradient existing between them. The process includes a free convection of humid air between the water and the inner surface of the glass. This process is dependent on the temperature differential between the condensing surface and water; this relationship can be represented by the following equation (6) [31, 32]:

$$Q_{c,wg} = h_{c,wg}\ A_b \left(T_w - T_g\right) \quad (6)$$

Where $hc_{,wg}$, can be expressed by equation (7) [31]:

$$h_{c,wg} = 0.884\left[\Delta T\right]^{1/3} \quad (7)$$

where ΔT represents the temperature difference between the condensing surface (Glass) and water, which can be written in terms of P_{water} and P_{glass}, which are the partial vapor pressures at the temperatures of the water and glass surfaces, respectively.

b) The radiation heat transfers between the water and the glass cover ($Q_{r, wg}$) can be expressed in terms of the equivalent radiation heat transfer coefficient (hr), as shown in equation (8) [30]:

$$Q_{r,wg} = h_{r,wg}\ A_w \left(T_w - T_g\right) \tag{8}$$

The coefficient representing radiative heat transfer from the water to the glass can be found from the Stefan-Boltzmann equation as follows [30]:

$$Q_{r,wg} = \varepsilon_{effective}\ \sigma \left(\frac{\left(T_w + 273.15\right)^2 + \left(T_g + 273.15\right)^2}{\left(T_g + T_w + 546.3\right)} \right) \tag{9}$$

Where:

σ: Stefane-Boltzmann constant (5.67×10^{-8})w/m^2 .K^4

A_w: The total area of the water basin surface (m^2)

ε effective: The effective radiative interaction parameter between the water surface and glass, which can be expressed by equation (10) [30]:

$$\varepsilon_{effective} = \frac{1}{\frac{1}{\varepsilon_w} + \frac{1}{\varepsilon_g}} - 1 \tag{10}$$

c) The evaporative thermal exchange occurring between the condensing surface and water ($Q_{e,wg}$): Inside the hot basin, water evaporates due to heat transfer, rising as water vapor, which then begins to condense on the glass surface, releasing heat. This mechanism reflects the energy loss due to the transition phase, and can be quantified as in equation (11) [33]:

$$Q_{e,wg} = h_{e,wg}\ A_w \left(T_w - T_g\right) \tag{11}$$

The evaporative thermal exchange occurring between the glass surface and water is correlated to the coefficient of convective heat transfer, as described by equation (12) [34]:

From equations (11) and (12), the coefficient of evaporative heat transfer from saline water to the condensing surface (glass cover),it can be written as in equation (13) [33]:

$$Q_{e,wg} = 0.01623 h_{c,wg}\ A_w \left(P_w - P_g\right) \tag{12}$$

$$h_{e,wg} = 0.01623 h_{c,wg} \left(\frac{P_w - P_g}{T_w - T_g} \right) \tag{13}$$

When solar energy strikes the surface of the receiver, it will raise the temperature of the receiver higher than the ambient temperature, then heat will suffer losses through radiation, convection, and water evaporation in the lower basin of the solar still, it can be represented by the equation (14) [34]:

$$Q_{per} = Q_{cv} + Q_{ray} + Q_{evap} \tag{14}$$

where, Q_{cv} is the heat losses by convection, Q_{ray} represents heat losses by radiation, and Q_{evap} is heat losses by water evaporation.

4.4. Electric system

Thermoelectric devices were used to study the generation of electricity by exploiting the temperature difference between the lower basin (heating basin) and the upper basin filled with water. The Peltier units were examined to investigate the effect of thermal variation on heat generation through two main concepts:

Firstly, the upper water basin was utilized for water desalination. The hot side of the Peltier unit groups was positioned on the external surface of the thermal condenser, while the cold side was oriented inside toward the water. To maintain operational stability and prevent material degradation, the setup was covered with an aluminum sheet.

Secondly, each assembly, consisting of four Peltier units, was positioned beneath the base of small aluminum basins filled with water (23 x 14 cm). The hot side of the assembly is placed in direct contact with the glass surface condenser to facilitate heat transfer and enhance evaporation performance. Figure 4 illustrates the mechanism of electricity generation using a Peltier device integrated with the two water basin.

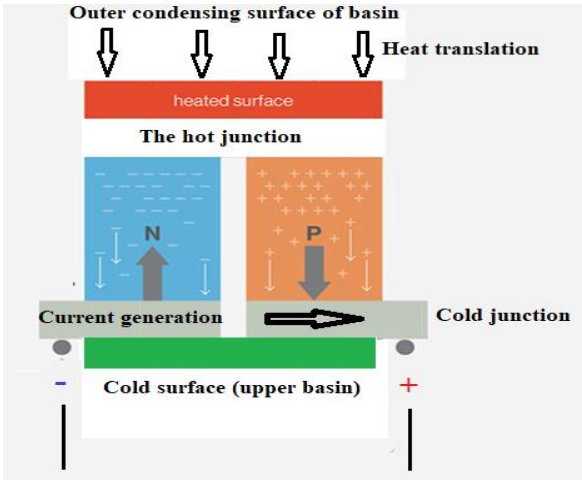

Figure 4. The current generation with temperature differences between the two sides

The heat transfer process begins from the hot side to the cold side of these systems (Peltier modules). The experiment is conducted from 8:30 AM to 3:30 PM. The voltage and temperature difference data are documented at intervals of 30 minutes to find the efficiency of the Peltier unit.

4.5. Data analysis and software

The experimental data collected were processed and analyzed using Microsoft Excel, which was employed for data organization, basic calculations, and preliminary plotting. Further graphical representation and detailed data analysis, including curve fitting and statistical evaluation, were performed using Origin 2023. These tools facilitated accurate interpretation of the experimental results.

5. Results and Discussion

5.1. The absorbed temperature

Solar radiation measurements were carried out from 8:00 AM to 3:30 PM in the study area, Iraq (Salah al-Din/Baiji), located at a latitude (35.018) and a longitude (43.445) during the last three days of August in 2025. Figure 5 shows the temporal variation of solar radiation intensity, showing relatively consistent values on clear days. Radiation intensity increased gradually in the morning reaching higher values between 12:00 PM and 3:00 PM. The peak solar radiation recorded was 970 w/m2, corresponding to the highest intensity period, and then begins to decrease. A similar study was conducted by the researcher [18].

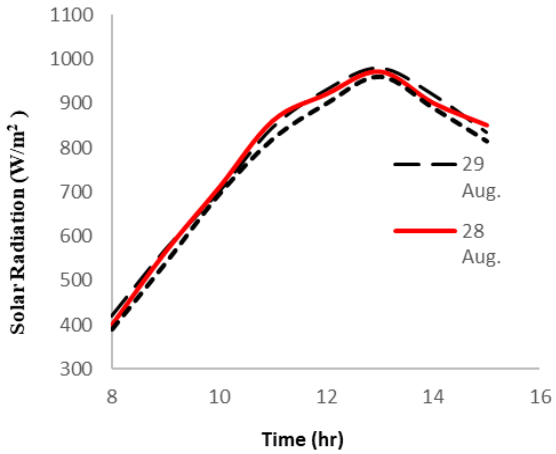

Figure 5. Solar radiation with local time, (28,29,30) August

The initial stage of the distillation process was conducted without an upper water basin, utilizing a glass condensing surface. The overall distillation efficiency was relatively low for several reasons, primarily due to the small temperature gradient between the heating basin and condensing surface, which resulted in limited heat transfer and reduced vapor generation. At the onset of the heating process, the rate of thermal absorption was minimal; however,as solar radiation increased, the evaporation rate correspondingly rose due to the absorbed energy by the receiver. This behavior represents a direct proportional relationship between evaporation and solar intensity; the same behavior was observed in previous studies [٣٣,3٠]. Figure 6 illustrates the relationship between the measured temperature as a function of time.

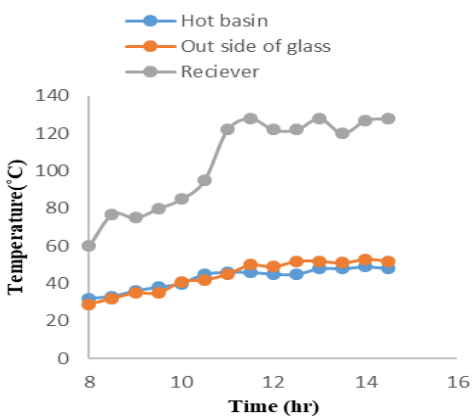

Figure 6. The relation between of measured temperature of the hot basin and time

In the second stage of the distillation process, a combined system consisting of a hot basin (lower basin) and a cold basin (upper basin) was utilized. The cold basin served initially as a water source for the hot basin. Peltier modules were installed on the upper basin to transfer heat from the hot basin to the upper basin. Figure 7 illustrates the thermal variation of the different parameters over time.

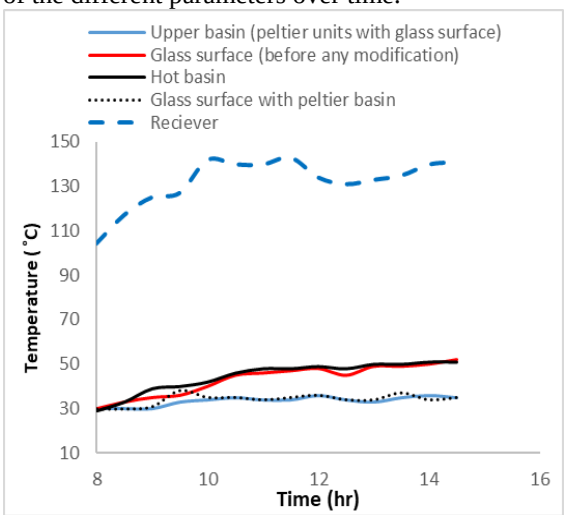

Figure 7.The relation between the measured temperatures with time

From Figure 7, it is evident that there is a temperature gradient exists between the hot basin and the upper basin, which contributes to enhancing the condensation process [8, 36]. In addition, the upper water temperature remained relatively stable throughout the day, with only a slight increase observed. In both cases, using a lower water basin alone or the upper water basin integrated with Peltier modules, the maximum temperature was recorded between 12:00 PM and 2:00 PM. Wind speed ranged between 2- 3.5 m/s, which is a significant factor influencing the desalination process [28].

The maximum temperatures of the lower and upper basins reached 52°C and 36 °C, respectively. The condensation surface temperatures were 49°C, 38°C, and 35°C for the system without the upper basin, with the upper basin, and with the upper basin coupled to the Peltier modules, respectively. It is evident that Peltier modules contributed to effective heat transfer from the condensing surface directly to the upper basin. The ambient temperature peaked between 12:30 PM and 3:00 PM, followed by a gradual decline.

5.2. The Water Productivity

The water production was evaluated before and after the installation of the upper basin. The volume of distilled water was measured from 8:30 AM to 3:30 PM, and which data was recorded at thirty-minute intervals. Figure 8 illustrates the relationship between desalinated water volume and time.

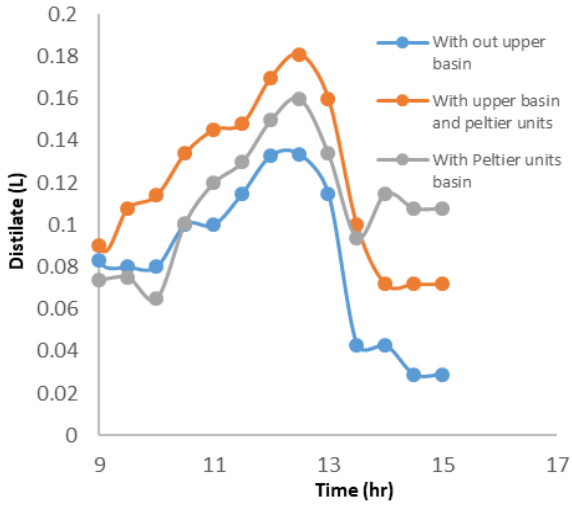

Figure 8. The amount of distilled water over time

During the early hours, water production was relatively low due to the limited amount of absorbed energy required for heating [37]. A noticeable increase began at around 10:30 AM. The modified configuration, which incorporated the upper basin as a water source, contributed to an increase in the extracted water volume as a result of the enhanced condensation rate on the glass surface. The maximum yield occurred between 12:00 PM and 3:00 PM, followed by a gradual decline. The maximum water yield was recorded between 12 PM and 1 PM, reaching approximately 0.479L/hour, corresponding to a thermal gradient of about 17˚C. The daily water yield of the distillation system without the upper basin, with an upper basin, and an upper basin integrated with Peltier modules was 0.8 L/ day, 1.328 L/day and 1.770 L/day respectively.

This corresponds to an improvement of approximately (1.770 L/day, 121%, and 1.385 L/day is 66%).In other words, the overall productivity of the modified system reached about 221% of that of the conventional system, indicating a more practical and feasible performance compared to previously reported studies. The daily collected water is influenced by many factors, including the temperature variations of the glass cover, the lower heating basin (distillation basin), solar center temperature, the ambient air temperature, the addition of the upper water basin and Peltier

modules, as well as the overall design conditions [38, 39].

Many studies have explored various ideas and methods to enhance and increase solar condensation using parabolic troughs. However, no previous research has investigated the use of an upper basin with a hot basin to assist in the condensation process. Furthermore, no study has examined the integration of Peltier units (modules) with solar distillation systems as electricity-generating units, which contribute to reducing the temperature of the condensing surface by transferring heat from the hot side of the Peltier units to the cold side, which in turn transfers it to the upper basin. Figure 9 illustrates the efficiency improvement achieved by the upper basin in combination with the Peltier units.

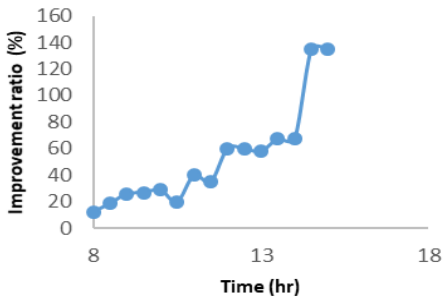

Figure 9. Efficiency improvement of distilled water

From Figure 9, the improvement in water yield is the highest between 12:00 and 3:00 PM, although the quantity of water collected after distillation water obtained was greater between 12:00 and 1:00 PM. This is because the liquid temperature peaks at that time due to the high amount of absorbed heat [40]. Furthermore, the temperature of the glass cover was significantly preserved, creating a high temperature difference between the hot water (heating basin) and the glass surface. Figure 10 shows the relation between the improvement ratio with solar radiation and ambient temperature.

The productivity of distilled water is in a state of upward and not a linear relationship, because the ambient conditions (solar radiation, wind speed) directly affect the performance of the solar still. The higher solar radiation intensity increases the productivity of the solar still [38, 40], due to the greater heat flux entering the desalination system, which raises the temperature of the hot basin and enhances the driving force for evaporation and condensation. Therefore, the increase in ΔT contributed to improving both distillation efficiency and productivity [42, 43]. Additionally, wind speed plays a significant role in determining heat losses, thereby reducing the thermal efficiency of the solar still.

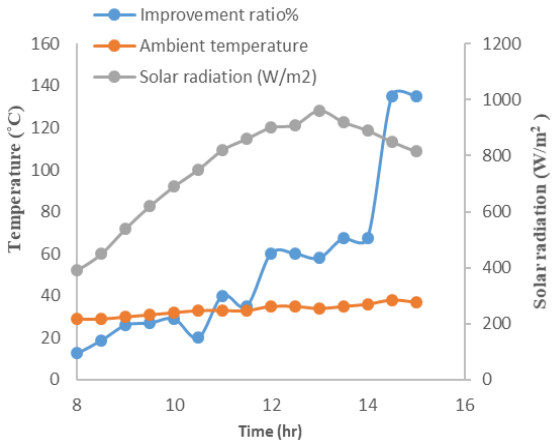

Figure 10. Improvement ratio with ambient temperature and solar radiation

5.3. The thermoelectricity generation

Readings were recorded every half hour, taking into account the temperature gradient between the hot and cold sides. Figure 11 illustrates the relationship between the generated voltage and time for the Peltier modules basin and the Peltier modules with an upper water basin. The hot side of the Peltier units absorbs heat from the outer surface of the condensing surface and transfers it to the cold side, where it is then released. An increase in the temperature difference between the two sides results in higher voltage generation. The temperature of the hot side of the Peltier unit rises, reaching its peak between high value at 12:00 PM to 2:30 PM before gradually declining. This behavior corresponds with the solar radiation intensity during the same period, as a higher solar radiation intensity leads to an increase in the temperature of the hot side of the thermoelectric units [44].

The voltage values obtained in the solar distillation experiment show differences in the values obtained in the two cases. Initially, individual basins distributed across the surface for each group of Peltier modules (4- Peltier modules) produced the highest recorded voltage of 3.456 volts. However, when the four separate basins were connected with (16-Peltier modules, the generated voltage increased to approximately 13.824 volts. The variation in voltage values is attributed to air movement, which occasionally causes localized or lateral cooling for the Peltier units' basin, thereby enhancing the generated voltage.

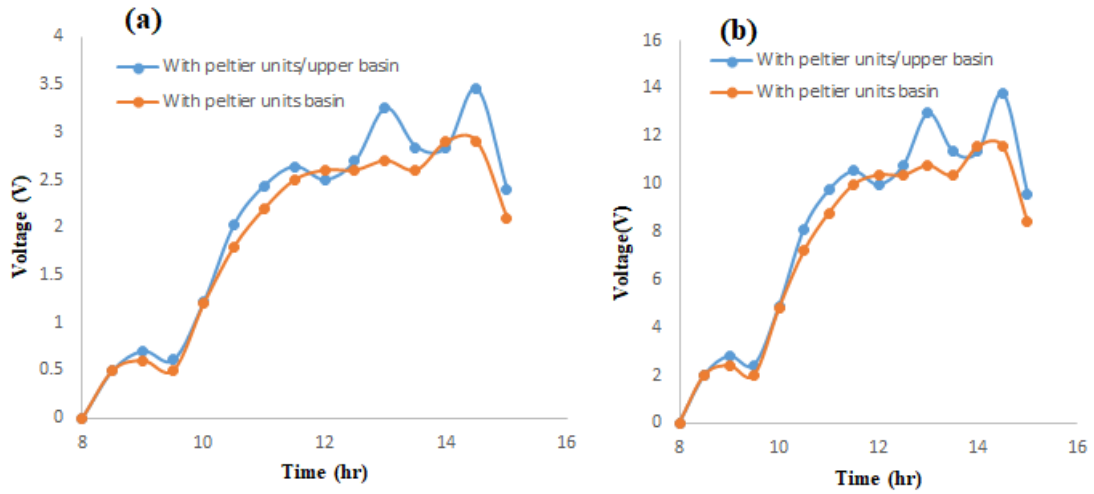

Figure 11. Voltage generation from distillation system: a) one-unit system (4 -Peltier units), b) four-unit system with upper basin (16- Peltier units)

The temperatures differ between both sides of the Peltier unit with respect to time, as depicted in Figure 12.

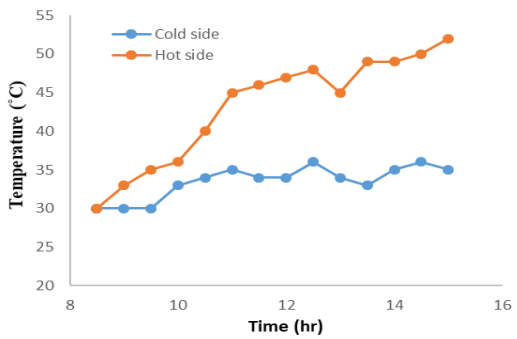

Figure 12. The temperatures of the cold and hot sides of the Peltier unit

The voltage increases by increasing the temperature gap between the two sides of the Peltier unit, it can be represented by equation (15) [23].

$$\Delta T = T_{hot\ side} - T_{cold\ side} \quad (15)$$

A

s shown in Figure 12, a temperature gradient is observed between the two faces of the Peltier unit. Increasing the temperature difference leads to an enhancement in the generated voltage. During the initial hours of the experiment, the temperature difference is relatively small, then gradually increases as the temperature of the hot basin increases. The maximum open voltage (V_{oc}) of four Peltier units (V) when the solar radiation intensity is maximum at noon, with the greatest difference in temperature value (ΔT= 17 ˚C), is 3.54 volts, and 13.82 volts for four Peltier groups with 16 units. at the same conditions. The obtained voltage is affected by the temperature gradient of 1ºC across the Peltier unit. The high Seebeck effect is due to the materials as a key parameter to increasing the efficiency of the Peltier module [44, 45]. Documented data demonstrates the effectiveness of Peltier units in transferring and dissipating heat from the hot side to the cold side. This is attributed to the internal structure of the Peltier unit, which consists of pairs of semiconductors connected in series, directing the heat flow. Each conductor within the Peltier module dissipates a specific amount of heat for every degree Celsius, thereby increasing the generated voltage. Consequently, the Peltier plates were effective in heat dissipation and voltage generation, supporting their use as an efficient technology for simultaneous thermal energy management [46, 47].

It is observed from Figure 13 that the generated voltage is directly proportional to the amount of water collected. The thermal gradient between the water temperature in the hot basin and the glass condensing surface influences both. However, the relationship exhibits fluctuations due to variation in absorbed heat values with both wind speed and the difference in heat transfer between the glass and the water. Moreover, the amount of water produced decreases sharply after 2:00 PM, while the generated voltage remains elevated until approximately 3:00 PM. This reduction in the collected water may be attributed to increased internal vapor pressure inside

the still, which reduces heat transfer, despite the temperature difference that simultaneously high heat output, and the generated voltage maintains its high level until 3:00 PM due to the generated thermal difference.

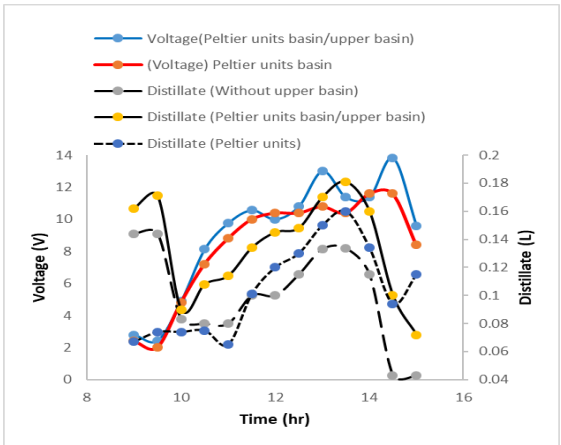

Figure 13. Variation of Voltage and distilled water with experimental period

5.4. Validating the Results of Voltage

A comprehensive validation of the present study was conducted by the performance of the thermoelectric modules with the data set of Cheng, et al. [48]. Our results are consistent and monotonic increase in the generated voltage with increasing temperature difference, confirming that the present experimental behavior follows the same thermoelectric trend in the literature, which is consistent in the overall direction of performance, providing the first level of validation for the obtained results.

The voltage measured in the present study (٢,٢٣٦ – 3.456 volts) for ΔT = (11-17 ˚C) is close to the commonly reported operational voltage for the TEC1-12706 model under the same thermal gradient. Despite the low difference in the generated voltage, both studies mentioned an appropriate increase in voltage with ΔT. This behavior indicates similar thermoelectric response characteristics within their respective thermal domains.

Cheng et al., [48] are utilized a passive energy harvesting method using commercial thermoelectric units, where a liquid-saturated top layer induces a temperature gradient (ΔT) through spontaneous evaporative cooling. Experimental tests on water, ethanol, acetone, and air showed that voltage output is highly dependent on the fluid's evaporation rate. The internal consistency of the experimental study is supported by the gradual increase in voltage across all examined ΔT values with no sudden fluctuations, this behavior refers to stable thermal boundary conditions, and reliable calculation procedures. Furthermore, the measured voltages agree with the theoretical expectations of the Seebeck coefficient of the TEC1-12706 module, reinforcing the scientific plausibility of the experimental results. The only distinction between the two outcomes lies in the fact that the researcher Cheng, et al., [48] are employed the thermal gradient was maintained through a self-driven evaporative cooling mechanism, in which the evaporative liquid extract latent heat from the thermoelectric upper surface, producing a sustained temperature difference relative to the lower surface, which remains stable at ambient temperature. In contrast, the design adopted in the present study relies entirely on clean energy without any water wastage or the use of harmful chemical cooling agents.

Table 2. The voltage generated with the thermal differences as comparing with same results [48]

Present study (four Peltier units) TEC1-12706		**Chen, et al. [48], (one Peltier unit) TEC1-12706**		
ΔT ˚C	Generating voltage (Volt)	ΔT ˚C	Generating voltage (V)	Cooling source
11	2.236	4.7	0.008	(water W-LEG)
12	2.2440	5.7	0.014	(e-LEG)
13	2.640	10.7	0.055	Acetone (a-LEG)
14	2.844	17	0.66	Air cooling
16	3.252	22-25	0.88	Water (LEGs)

Based on the results presented in the table 2, the maximum output voltage obtained from a single peltier unit reaches approximately (0.88 Volt) at a temperature gradient of 22-25 ˚C when employing water evaporation as the cooling mechanism. In contrast, using air cooling yielded a lower maximum voltage of (0.66volt) at a temperature difference of roughly 17˚C for a single peltier unit. The present study, observes aconsistent trend when operating four peltier under a thermal gradient of (16˚C) at a total voltage of (3.252 volt) was generated, resulting in an average output of approximately (≈ 0.813 volt) per peltier unit.

6. Limitations and Future Work

This study was subjected to several limitations: simplified assumptions were used; measurements were conducted under specific climatic conditions that may not be representative of all regions in Iraq; additionally, only a limited number of thermoelectric units were employed, covering only a small portion of the condensation surface. The future implementation and production of this design represents a shift in the field of desalination and electrical power generation if high-performance thermoelectric units are used. According to the obtained results, it is considered suitable for application in most countries with high solar radiation availability, with Iraq being a primary example. In addition, it is possible to work on such a design in the future with bigger sizes, enhanced heating, and elimination of issues related to the solar still, as previously mentioned.

7. Conclusion

The performance of the solar stills suffers from limited fresh water, low thermal efficiency, gradual reduction of solar energy input over time due to the dust accumulation, and Poor evaporation–condensation mechanism. These challenges restrict the practical applicability of solar distillation system design, particularly in regions with water demand. The motivation behind this study was to reduce the challenges associated with solar stills, in addition to developing a design that ensures energy generation in regions lacking it or experiencing frequent interruptions of energy.

1- The technical contributions of this recent research paper include the addition of an upper basin that serves as a water source for the lower basin and acts as a cooling device for the glass condenser to contribute to condensation and electrical power generation when using large thermoelectric generators.

2-Experimental studies confirm that the use of the upper basin has contributed to increasing the efficiency and productivity of distilled water by enhancing the condensation process to high levels, in addition to enhancing the efficiency of the Peltier units through the thermal differential between the two basins. Water productivity has more than doubled (121%, 66%) when using this design with the proposed modifications, with free electricity savings.

3-The maximum water yield was recorded between 12:00 PM and 1:00 PM, reaching approximately (0.479L /hour), corresponding to a thermal gradient of about 17˚C.

4- The obtaining voltage was (13.83 V) using four Peltier basin groups (16 units) ,which is relatively acceptable and can be increased to higher values by increasing the thermal temperature of the lower basin.

Acknowledgments

This work was completed with the support of the research group, with assistance from the Ministry of

Education, College of Engineering/Tikrit University, Iraq.

Nomenclature

A_a	Aperture Area
A_{rec}	Receiver Area
A_w	Surface Area of Water Basin
CR-opt	Optical Concentration Ratio
CR	Geometric Concentration Ratio
d	Diameter of Parabolic Concentrator
$Exergy_{out}$	Exergy Efficiency
$Exergy_{in}$	Exergy efficiency
f	Focal Distance
h	Depth of Parabola
$h_{r,wg}$	Heat transfer coefficient (Glass and water)
I_{sur}	Incident Solar Radiation
I_{rec}	Reflected Solar Radiation on Receiver
$\varepsilon_{effective}$	Effective Emissivity
ε_g	Glass Emissivity
P_w	Partial Pressure of Water
P_g	Partial Pressure of Glass
$Q_{c.wg}$	Convective Heat Transfer Rate (Glass and water)
$Q_{r,wg}$	Radiation Heat Transfer (Glass and water)
Q_{per}	Total Teat Transfer Looses
Q_{cv}	Heat Losses by Convection
Q_{evap}	Heat Loose by Evaporation
Q_{rad}	Heat losses by Radiation
T_{water}	Temperature of Water
T_{glass}	Temperature of Glass
ΔT	Temperature Difference
T_w	Water Temperature
T_g	Glass Temperature
$\eta_{exergy,hourly}$	Hourly Exergy Efficiency
σ	Stefan-Boltzmann Constant

References

1. Resen, I. S., Skheel, O. R., Al-Obaidi, M. A., Al-Musawi, S. S., & Hydrose, A. (2025). Augmentation of Solar Air Heater Performance by Experimental Modification. *Journal of Solar Energy Research*, *10*(3), 2491-2500. https://doi.org/10.22059/jser.2025.402707.1639
2. Nazar, M., Saleem, A. M., & Alomar, O. R. (2024). Development of Compound Parabolic Concentrator based on Flat Plate Receiver Solar Air Heater and Phase Change Material. *NTU Journal of Renewable Energy*, *6*(1), 1-9. https://doi.org/10.56286/ntujre.v6i1.642
3. Nakade, A., Aglawe, A., More, K., & Kalbande, V. P. (2024). Experimental analysis of two stage solar still integrated with thermal storage based solar collector using nano-enhanced phase change materials. *Desalination and Water Treatment*, *320*, 100755. https://doi.org/https://doi.org/10.1016/j.dwt.2024.100755
4. Chinnappan, T., C.M, R., Dhairiyasamy, R., & Rajendran, S. (2024). Comparative Analysis of Polycarbonate and Glass Cover Configurations for Enhanced Thermal Efficiency in Flat Plate Solar Collectors for Water Heating. *Journal of Solar Energy Research*, *9*(1), 1794-1810. https://doi.org/10.22059/jser.2024.374268.1394
5. Aboulfotoh, A. M., Heikal, G. E., Abdo, A., & khadiga, y. e. g. (2023). Solar distillation Systems Design and Enhancements Review. *The Egyptian International Journal of Engineering Sciences and Technology*, *43*(1), 1-18. https://doi.org/10.21608/eijest.2022.150949.1178
6. Thabit, Q., Nassour, A., & Nelles, M. (2022). Innovative hybrid waste to energy–parabolic trough plant for power generation and water desalination in the Middle East North Africa region: Jordan as a case study. *Energy Reports*, *8*, 13150-13169. https://doi.org/https://doi.org/10.1016/j.egyr.2022.09.144
7. Abdullah, A. S., Omara, Z. M., Alarjani, A., & Essa, F. A. (2021). Experimental investigation of a new design of drum solar still with reflectors under different conditions. *Case Studies in Thermal Engineering*, *24*, 100850. https://doi.org/https://doi.org/10.1016/j.csite.2021.100850
8. Hyal, L. S., Jalil, J. M., & Hanfash, A. O. (2024). Enhancing the solar still performance using different designs of

absorber with heat storage materials and different wick materials: A review. *Engineering and Technology Journal*, *42*(1), 33-50. https://doi.org/10.30684/etj.2023.139522.1435

9. Madhuri, R. V. S., Said, Z., Ihsanullah, I., & Sathyamurthy, R. (2025). Solar energy-driven desalination: A renewable solution for climate change mitigation and advancing sustainable development goals. *Desalination*, *602*, 118575. https://doi.org/https://doi.org/10.1016/j.desal.2025.118575
10. Kalidasan, B., Divyabharathi, R., Pandey, A. K., Subramaniyan, C., & Mohankumar, S. (2021). Technological Advancement of Solar Thermal System Desalination Process – A Review. *IOP Conference Series: Materials Science and Engineering*, *1059*(1), 012061. https://doi.org/10.1088/1757-899X/1059/1/012061
11. Diab, M. R., Abou-Taleb, F. S., & Essa, F. A. (2022). Effect of basin water depth on the performance of vertical discs' solar still—experimental investigation. *Environmental Science and Pollution Research*, *29*(60), 91368-91380. https://doi.org/10.1007/s11356-022-22220-8
12. Dawoud, M. A., Sallam, G. R., Abdelrahman, M. A., & Emam, M. (2024). The Performance and Feasibility of Solar-Powered Desalination for Brackish Groundwater in Egypt. *Sustainability*, *16*(4), 1630. https://doi.org/10.3390/su16041630
13. Sasongko, S. B., Sanyoto, G. J., & Buchori, L. (2021). Study of Performance: An Improved Distillation Using Thermoelectric Modules. *Chemical Engineering Transactions*, *89*, 649-654. https://doi.org/10.3303/CET2189109
14. Ashour, A. M., Kadhim, S. A., Al-Ghezi, M. K. S., Omle, I., & Sathyamurthy, R. (2025). Performance analysis of a water desalination system using humidification and dehumidification techniques with thermoelectric cooling unit. *Case Studies in Thermal Engineering*, *73*, 106671. https://doi.org/https://doi.org/10.1016/j.csite.2025.106671
15. Al-Madhhachi, H., & Min, G. (2017). Effective use of thermal energy at both hot and cold side of thermoelectric module for developing efficient thermoelectric water distillation system. *Energy Conversion and Management*, *133*, 14-19. https://doi.org/https://doi.org/10.1016/j.enconman.2016.11.055
16. Al-Madhhachi, H. (2018). Effective Thermal Analysis of Using Peltier Module for Desalination Process. *Advances in Science, Technology and Engineering Systems Journal*, *3*(1), 191–197. https://doi.org/10.25046/aj030122
17. Hasanzadeh, H., Mohammadi, S., Shafii, M. B., & Daneshvar, M. (2025). Designing and constructing a solar thermal water desalination system: Evaluating the role of thermoelectric in enhancing evaporation and condensation process. *Next Energy*, *9*, 100388. https://doi.org/https://doi.org/10.1016/j.nxener.2025.100388
18. Mohammed Ajmi, A., & Alaa, Y. A. (2025). Effect of Innovative Glassy House and Secondary Reflectors Combination with Nanocoating on Fast and Slow Increase of Receiver Temperature in Parabolic Solar Collector. *Eximia*, *14*(1), 104-116. https://doi.org/10.47577/eximia.v14i1.534
19. Aqlan, A. M., Aklan, M., & Momin, A. E. (2021). Solar-powered desalination, a novel solar still directly connected to solar parabolic trough. *Energy Reports*, *7*, 2245-2254. https://doi.org/https://doi.org/10.1016/j.egyr.2021.04.041
20. Guo, D., Sheng, Q., Dou, X., Wang, Z., Xie, L., & Yang, B. (2020). Application of thermoelectric cooler in temperature control system of space science experiment. *Applied Thermal Engineering*, *168*, 114888. https://doi.org/https://doi.org/10.1016/j.applthermaleng.2019.114888
21. Tian, M.-W., Aldawi, F., Anqi, A. E., Moria, H., Dizaji, H. S., & Wae-hayee, M. (2021). Cost-effective and performance analysis of thermoelectricity as a building cooling system; experimental case study based on a single TEC-12706 commercial module. *Case Studies in Thermal Engineering*, *27*, 101366.

https://doi.org/https://doi.org/10.1016/j.csite.2021.101366

22. El Ghetany, H. H., Elgohary, H. M., & Mohammed, Y. M. (2021). Performance Improvement of Solar Water Distillation System Using Nanofluid Particles. *Egyptian Journal of Chemistry*, *64*(8), 4425-4431. https://doi.org/10.21608/ejchem.2021.64067.3372
23. Lin, L., Zhang, Y.-F., Liu, H.-B., Meng, J.-H., Chen, W.-H., & Wang, X.-D. (2019). A new configuration design of thermoelectric cooler driven by thermoelectric generator. *Applied Thermal Engineering*, *160*, 114087. https://doi.org/https://doi.org/10.1016/j.applthermaleng.2019.114087
24. Kharmouch, A., Hasan, M. K., Sabik, E. Y., Bouali, H., Mamur, H., & Bhuiyan, M. R. (2025). Numerical Optimization of Multi-Stage Thermoelectric Cooling Systems Using Bi2Te3 for Enhanced Cryosurgical Applications. *Thermo*, *5*(3), 22. https://doi.org/10.3390/thermo5030022
25. Talugeri, V., Pattana, N. B., Nasi, V. B., Shahapurkar, K., Soudagar, M. E. M., Ahamad, T., Kalam, M. A., Chidanandamurthy, K. M., Mubarak, N. M., & Karri, R. R. (2023). Experimental investigation on a solar parabolic collector using water-based multi-walled carbon-nanotube with low volume concentrations. *Scientific Reports*, *13*(1), 7398. https://doi.org/10.1038/s41598-023-34529-6
26. Hassan, H. M. A., Amjad, M., Tahir, Z. u. R., Qamar, A., Noor, F., Hu, Y., Yaqub, T. B., & Filho, E. P. B. (2022). Performance analysis of nanofluid-based water desalination system using integrated solar still, flat plate and parabolic trough collectors. *Journal of the Brazilian Society of Mechanical Sciences and Engineering*, *44*(9), 427. https://doi.org/10.1007/s40430-022-03734-1
27. Shilpa, M. K., Raheman, M. A., Aabid, A., Baig, M., Veeresha, R. K., & Kudva, N. (2023). A Systematic Review of Thermoelectric Peltier Devices: Applications and Limitations. *Fluid Dynamics \& Materials Processing*, *19*(1). https://doi.org/10.32604/fdmp.2022.020351
28. Alshqirate, A. A., Badran, O., Quran, O., Al-Marahleh, G., Olimat, A. N., Al Alawin, A., Shorman, A. A., & Alahmer, A. (2024). Enhanced distilled water productivity using an innovative semi-cylindrical tent-shaped solar still coupled with evacuated tubes. *International Journal of Thermofluids*, *24*, 100880. https://doi.org/https://doi.org/10.1016/j.ijft.2024.100880
29. Muthiah, C., Subramani, S., & Murugan, D. K. (2023). Productivity enhancement of solar stills using natural fibers: experimental investigation on the effect of Strychnos potatorum seeds and gooseberry stems. *Desalination and Water Treatment*, *310*, 12-22. https://doi.org/https://doi.org/10.5004/dwt.2023.29962
30. Mahgoub, A. A., Elsherbiny, S. M., El-Masry, O. A. A., & Elsamni, O. A. (2025). Enhanced distillate production of stepped solar still via integration with multi-stage membrane distillation. *Scientific Reports*, *15*(1), 12541. https://doi.org/10.1038/s41598-025-95098-4
31. Haghighat, M., Entezarian, M. M., Salimi, M., & Amidpour, M. (2025). Exploring interfacial solar evaporation heat transfer mechanisms of photothermal solar still systems. *Case Studies in Thermal Engineering*, *68*, 105883. https://doi.org/https://doi.org/10.1016/j.csite.2025.105883
32. Touaref, F., Saadi, A., Farkas, I., & Seres, I. (2025). Design and implementation of parabolic trough solar concentrator distiller. *Energy Reports*, *13*, 1138-1157. https://doi.org/https://doi.org/10.1016/j.egyr.2025.01.001
33. Jamil, F., Hassan, F., Shoeibi, S., & Khiadani, M. (2023). Application of advanced energy storage materials in direct solar desalination: A state of art review. *Renewable and Sustainable Energy Reviews*, *186*, 113663. https://doi.org/https://doi.org/10.1016/j.rser.2023.113663
34. Khalaf, M. O., Özdemir, M. R., & Sultan, H. S. (2025). A Comprehensive Review of Solar Still Technologies and Cost: Innovations in Materials, Design, and Techniques for Enhanced Water

Desalination Efficiency. *Water*, *17*(10), 1515. https://doi.org/10.3390/w17101515

35. Muftah, A. K., Zili-Ghedira, L., Abugderah, M. M., Hassen, W., Becheikh, N., Alshammari, B. M., & Kolsi, L. (2025). Sustainable Water Production: Solar Energy Integration in Multi-Effect Desalination Plants. *Water*, *17*(5), 647. https://doi.org/10.3390/w17050647
36. Wahab, A., Javid, W., Ahmed, H., Sheikh, A., Shahbaz, M., & Iqbal, S. (2024). Enhancing Fresh Water Production in Solar Parabolic Dish Desalination System. *Materials Proceedings*, *17*(1), 22. https://doi.org/10.3390/materproc2024017022
37. Shariah, A., & Hasan, E. (2023). Design of a new static solar concentrator with a high concentration ratio and a large acceptance angle based on bifacial solar cells. *Clean Energy*, *7*(3), 509-518. https://doi.org/10.1093/ce/zkac068
38. Muftah, A. F., Alghoul, M. A., Fudholi, A., Abdul-Majeed, M. M., & Sopian, K. (2014). Factors affecting basin type solar still productivity: A detailed review. *Renewable and Sustainable Energy Reviews*, *32*, 430-447. https://doi.org/https://doi.org/10.1016/j.rser.2013.12.052
39. Pisitsungkakarn,S.S.-h.,& Thomrungpiyathan, T. (2025). Evaluation of thermal efficiency in ethanol distillation by solar concentrating parabolic collector. *Case Studies in Thermal Engineering*, *66*, 105779. https://doi.org/https://doi.org/10.1016/j.csite.2025.105779
40. Al_qasaab, M. R., Abed, Q. A., & Abd Al-wahid, W. A. (2021). ENHANCEMENT THE SOLAR DISTILLER WATER BY USING PARABOLIC DISH COLLECTOR WITH SINGLE SLOPE SOLAR STILL. *Journal of Thermal Engineering*, *7*(4), 1000-1015. https://doi.org/10.18186/thermal.931352
41. Kadhim, S. A., Rashid, F. L., Hammoodi, K. A., Togun, H., Bouabidi, A., Askar, A. H., & Hussein, A. K. (2025). Performance enhancement of a single slope solar still using wick materials: A comparative experimental investigation with energy, exergy, and economic analysis. *Scientific African*, *28*, e02733. https://doi.org/https://doi.org/10.1016/j.sciaf.2025.e02733
42. Atta, A. E., Shehata, N., Mohamed, H. F. M., & Ali, M. R. O. (2021). A novel merging solar parabolic collector with thermoelectric generator using geothermal energy. *IOP Conference Series: Materials Science and Engineering*, *1046*(1), 012019. https://doi.org/10.1088/1757-899X/1046/1/012019
43. Freire, L. O., Navarrete, L. M., Corrales, B. P., & Castillo, J. N. (2021). Efficiency in thermoelectric generators based on Peltier cells. *Energy Reports*, *7*, 355-361. https://doi.org/https://doi.org/10.1016/j.egyr.2021.08.099
44. Shin, H.-C., & Pyun, S.-I. (2021). Some remarks on the Peltier heat in the thermoelectric phenomena. *Journal of Solid State Electrochemistry*, *25*(12), 2737-2746. https://doi.org/10.1007/s10008-021-05019-4
45. Lv, S., Ji, Y., Qian, Z., He, W., Hu, Z., & Liu, M. (2021). A novel strategy of enhancing sky radiative cooling by solar photovoltaic-thermoelectric cooler. *Energy*, *219*,119625. https://doi.org/https://doi.org/10.1016/j.energy.2020.119625
46. Radulov, A., Dechev, M., & Matsankov, M. (2025). Investigation of the Efficiency of a Peltier Element. *Engineering Proceedings*, *100*(1), 8. https://doi.org/10.3390/engproc2025100008
47. Korprasertsak, N., & Leephakpreeda, T. (2024). Maximizing cooling/heating performance of thermoelectric modules across variable thermal loads via optimal control based on COP curves. *Heliyon*, *10*(1). https://doi.org/10.1016/j.heliyon.2024.e24063
48. Cheng, P., Wang, D., & Schaaf, P. (2022). Simple and sustainable electric power generation by free evaporation of liquids from the surface of a conventional thermoelectric generator. Sustainable Energy & Fuels, 8(21), 4956–4961. https://doi.org/10.1039/d4se01156b